$$G = \begin{bmatrix} \# & 0 & 0 & 0 & 0 & 0 \\ 0 & \# & 0 & 0 & 0 & 0 \\ 0 & 0 & \# & 0 & 0 & 0 \\ 0 & 0 & 0 & \# & 0 & 0 \\ 0 & 0 & 0 & 0 & \# & x \\ 0 & 0 & 0 & 0 & x & \# \end{bmatrix}$$

$$H = \begin{bmatrix} \# & x & 0 & 0 & 0 & 0 \\ x & \# & 0 & 0 & 0 & 0 \\ 0 & 0 & \# & x & 0 & 0 \\ 0 & 0 & x & \# & 0 & 0 \\ 0 & 0 & 0 & 0 & \# & 1 \\ 0 & 0 & 0 & 0 & 0 & \# \end{bmatrix}$$

$$C = \begin{bmatrix} \# & 0 & 0 & 0 & 0 & 0 \\ 0 & \# & 0 & 0 & 0 & 0 \\ x & x & \# & 1 & x & x \\ x & x & 0 & \# & x & x \\ 0 & 0 & 0 & 0 & \# & 0 \\ 0 & 0 & 0 & 0 & 0 & \# \end{bmatrix}.$$

After generating the initial population—Universal and Kernel chromosomes—the Kernel chromosome is checked for the infeasibility of the schema. Once all checks are cleared, the genetic process gets started. The process can be stopped as early as the first feasible chromosome is generated, or whenever the time limit is surpassed. The methodology presented in this paper is implemented on *DesignCPN*[1] [12] with code segments written in *ML* and with the logic of the process embedded in the colored Petri net model. An ML program can be used to transform or decode the bit string representation of an organization structure to its Petri net representation. The methodology is applied to the illustrative example: the algorithm yielded the first feasible chromosome in the fourth population. Fig. 7 shows the Petri net representation of this structure; overall, 30 populations were generated before the process was terminated by the user. The best structure in the 30th population is shown in Fig. 8 in terms of its Petri net representation. The structure in Fig. 7 is important in the sense that it was eliminated from the solution space by the hierarchical methodology in [3] because of the design decisions taken at an earlier stage by the designer. The results of the application of the methodology to the illustrative example are summarized in Figs. 9–11.

VII. Conclusions

A methodology for generating DIS architectures using a genetic algorithm has been presented. The approach provides an alternative for the generation of large-scale organizational structures where the combinatorial nature of the problem makes the previous approaches computationally expensive or infeasible. Another advantage of using the approach is that additional structural and performance criteria can be made an integral part of the design algorithm to direct the search for the solution in a particular direction.

References

[1] P. A. Remy and A. H. Levis, "On the generation of organizational architectures using Petri nets," in *Advances in Petri Nets 1988*, G. Rozenberg, Ed. Berlin, Germany: Springer-Verlag, pp. 371–385.

[2] S. K. Andreadakis and A. H. Levis, "Synthesis of distributed command and control for the outer air battle," in *Proc. 1988 Symp. Command Contr. Res.* McLean, VA: Sci. Applicat. Int. Corp., pp. 352–364.

[3] A. K. Zaidi and A. H. Levis, "Algorithmic design of distributed intelligence system architectures," in *Intelligent Control Systems: Theory and Practice*, M. M. Gupta and N. K. Sinha, Eds. Piscataway, NJ: IEEE Press, 1994.

[4] M. Minsky, *The Society of Mind*. New York: Simon & Schuster, 1986.

[5] A. H. Levis, N. Moray, and Baosheng Hu, "Task allocation models and discrete event systems," *Automatica*, vol. 30, Feb. 1994.

[6] A. H. Levis, "A colored Petri net model of intelligent nodes," in *Robotics and Flexible Manufacturing Systems*, J. C. Gentina and S. G. Tzafestas, Eds. Amsterdam, The Netherlands: Elsevier, 1992.

[7] M. D. Mesarovic, D. Macko, and Y. Takahara, *Theory of Hierarchical, Multilevel Systems*. New York: Academic, 1970.

[8] L. Davis, *Handbook of Genetic Algorithms*. New York: Van Nostrand Reinhold, 1991.

[9] J. H. Holland, *Adaptation in Natural and Artificial Systems*. Ann Arbor, MI: Univ. of Michigan Press, 1975.

[10] T. Murata, "Petri nets: properties, analysis and applications," *Proc. IEEE*, vol. 77, pp. 541–579, Apr. 1989.

[11] W. Reisig, *Petri Nets, An Introduction*. Berlin, Germany: Springer-Verlag, 1985.

[12] *Design/CPN: A Reference Manual*. Cambridge, MA: Meta Softw. Corp., 1992.

Auditory Guidance with the *Navbelt*—A Computerized Travel Aid for the Blind

Shraga Shoval, Johann Borenstein, and Yoram Koren

Abstract—A blind traveler walking through an unfamiliar environment and a mobile robot navigating through a cluttered environment have an important feature in common: both have the kinematic ability to perform the motion, but they are dependent on a sensory system to detect and avoid obstacles. This paper describes the use of a mobile robot obstacle avoidance system as a guidance device for blind and visually impaired people. Just as electronic signals are sent to a mobile robot's motion controllers, auditory signals can guide the blind traveler around obstacles, or alternatively, they can provide an "acoustic image" of the surroundings. The concept has been implemented and tested in a new travel aid for the blind, called the *Navbelt*. The *Navbelt* introduces two new concepts to electronic travel aids (ETA's) for the blind: it provides information not only about obstacles along the traveled path, but also assists the user in selecting the preferred travel path. In addition, the level of assistance can be automatically adjusted according to changes in the environment and the user's needs and capabilities Experimental results conducted with the *Navbelt* simulator and a portable experimental prototype are presented.

Index Terms— Auditory system, computer-aided instruction, handicapped aids, headphones, sonar navigation.

I. Introduction

In order for a blind person to follow a particular route, the person must have some concept or plan of that route. Once a route has been learned (by experience or verbal instructions), successful travel

requires the individual to be able to: 1) detect and avoid obstacles, 2) know their position and orientation, and, if necessary, 3) make corrections. The performance of both tasks can be enhanced through *electronic travel aids* (ETA's). Among commonly used ETA's are the *C5 Laser Cane,* the *Mowat Sensor,* the *Nottingham Obstacle Detector,* the *Binaural Sonic Aid,* the *Talking Signs,* and the *Sona System.*

The motion of a blind traveler in an unfamiliar environment is somewhat similar to that of a mobile robot. Both have the physical ability to perform the motion, but they are dependent on a sensory system to detect obstacles in the surroundings. Applying a mobile robot obstacle avoidance system in a travel aid for the blind introduces several new advantages to electronic devices. Using multiple ultrasonic sensors that face in different directions frees the user from the need to scan the surroundings manually. Furthermore, no additional measurement is required when an obstacle is detected, since its relevant dimensions are determined simultaneously by the multisensor system. In addition, the obstacle avoidance system can guide the blind traveler toward a target while avoiding obstacles along the path.

The transfer of mobile robot technology is a new approach in the development of ETA's for the blind. Robots have already been used in the past to assist blind travelers (i.e., the *Guide Robot Dog* [12]). However, in these applications mobile robot technology is **applied** (rather than transferred) to assist the blind, and the user acts as an operator to the device. Technology **transfer**, on the other hand, is more demanding as the expertise of a blind traveler and mobile robot technologies are combined, and the user is an integral part of the whole system.

All current ETA's for the blind either detect objects along the travel path (i.e., the *Laser Cane, Mowat Sensor, Sonicguide*), or provide a global navigation aid (i.e., the *Talking Signals, Talking Map, Gilden Device*). However no ETA can provide both tasks simultaneously. Furthermore, no travel aid for the blind can provide obstacle detection and avoidance. Mobile robot technology can integrate obstacle detection and global navigation to provide safe and reliable travel in an unfamiliar environment.

II. THE *Navbelt*

Based on our experience with obstacle avoidance for mobile robots [5], we have developed a new travel aid for the blind, called the *Navbelt* [3], [10]. The *Navbelt* consists of a belt, a portable computer, and ultrasonic sensors. In this system, the computer processes the signals that arrive from the sensors and applies the obstacle avoidance algorithm. The resulting signals are relayed to the user by stereophonic headphones, using a stereo imaging technique. The similarity between this approach and the original mobile robot application is illustrated in Fig. 1. The electrical signals that originally guided the robot around the obstacles are replaced by acoustic (or tactile) signals.

The *Navbelt* is designed for two operational modes.

1) Guidance Mode: The acoustic signals actively guide the user around obstacles in pursuit of the target direction. The signals carry information regarding the recommended direction and speed of travel as well as information about the proximity to obstacles.

2) Image Mode: This mode presents the user with an *acoustic panoramic image* of the environment by using stereophonic effects: sound signals appear to sweep through the user's head from the right ear to the left. The direction to an obstacle is indicated by the perceived spatial direction of the signal, and the distance is represented by the signal's volume.

To reduce the occurrence of erroneous readings due to noise, specular reflection, or crosstalk, we have integrated a noise reduction algorithm, known as Error Eliminating Rapid Ultrasonic Firing
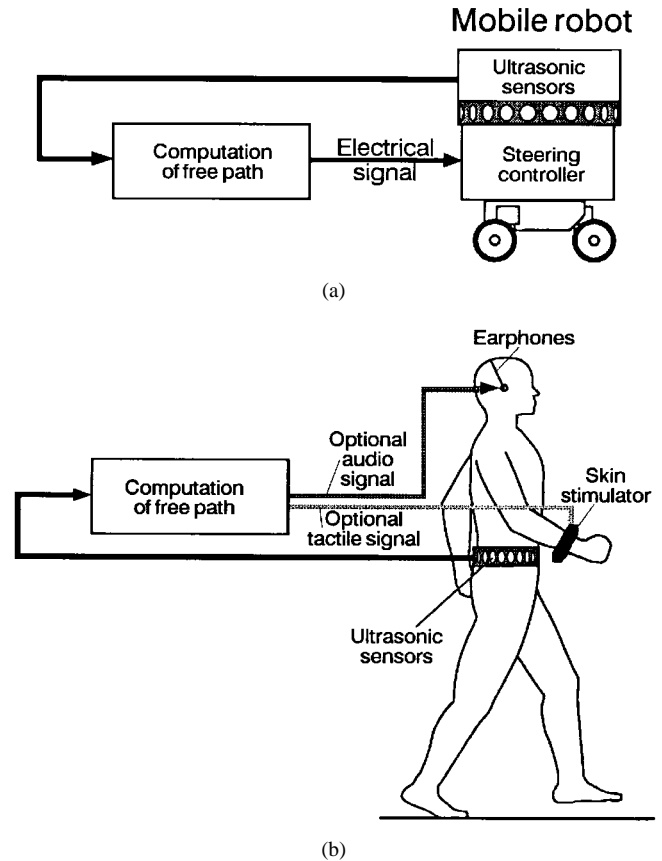

Fig. 1. Transfer of technology: mobile robot obstacle avoidance applied as a mobility aid for the blind.

(EERUF) [4]. EERUF allows multiple sonars to fire at rates that are five to ten times faster than those attained with conventional ultrasonic firing methods. At the same time, EERUF reduces the number of erroneous readings by one to two orders of magnitude. In addition, a low-pass filter is applied to further reduce the affect of inaccurate sonar readings. The EERUF method is implemented in the *Navbelt* as follows.

1) EERUF controls the ultrasonic sensors by scheduling the firing of each sonar and filters erroneous readings before they are processed by the obstacle avoidance algorithm.

2) The world model is divided into eight sectors, each representing one sonar. The angular width of the sectors is similar to that of the ultrasonic wave cone (approximately $15°$). Based on each sonar's reading, the corresponding sector is filled with the range to an obstacle. The sector range is updated as soon as a reliable reading is accepted by the EERUF control.

3) A polar obstacle density graph (H_i, $i = 1$–8) is then constructed from the sectorial map. The value of each sector in the polar histogram is calculated inversely proportional to the distance of the object of the corresponding sector, and it is statistically averaged with previous values of the same sector and with neighboring sectors. This statistical procedure is performed to further increase the data robustness to erroneous sonar readings.

4) The recommended travel direction is computed from the polar graph in an identical method to the one that was introduced in the vector field histogram (VFH) obstacle avoidance method for mobile robots [5].
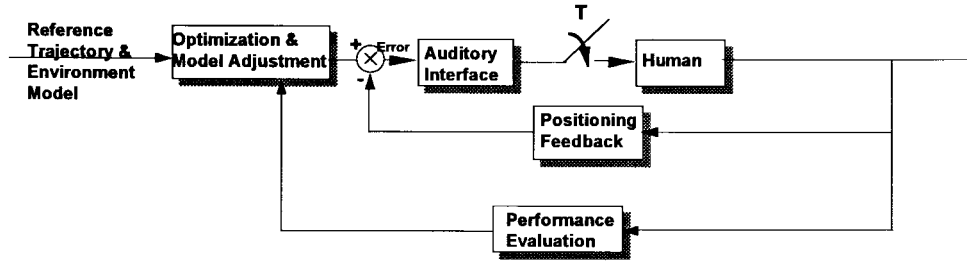
Fig. 2.   Adaptive information transfer for auditory signals.

A major concern of blind users, as revealed by a survey about the use of existing ETA's [2], was that too little information was acquired for the effort involved. In addition, blind travelers are concerned that acoustic signals may occlude external acoustic cues, which are very important to their confidence. To reduce these concerns, an **adaptive information control** system was implemented in the *Navbelt*. Fig. 2 describes the architecture of this system. The method requires a model of the user and the environment as well as the evaluation of the human performance. The *Optimization* module filters and formats the information and relays it to the user via the auditory interface (stereophonic headphones). The function of the optimization module is to relay the minimum amount of information that guarantees safe travel. This way the conscious effort required from the traveler is reduced, and the occlusion of external acoustic signals is minimized.

The optimization of the information flow is based on up-to-date models of the human and of the environment. The human model is based on McRuer's crossover model [9]. The most general presentation of this model is given by

$$G_c(s) = \frac{Ke^{-sD}(1 + T_a s)}{(1 + T_1 s)(1 + T_2 s)}. \tag{1}$$

D transportation lag (delays due to human reaction time);
K crossover frequency (sensitivity to the incoming signals);
T_1 smoothing lag time constant;
T_2 short neuromuscular delay;
T_a anticipation time.

Vinje [13] showed that for aural compensatory tracking the model can be simplified to

$$G_c(s) = \frac{Ke^{-sD}}{s}. \tag{2}$$

The environment model is calculated by the obstacle avoidance system and represents the complexity of the environment as perceived by the ultrasonic sensors [11]. This model is given by

$$E(s) = \sum_{i=1}^{8} H_i + \sum_{i=1}^{8} \frac{\partial(H_i)}{di} + \sum_{i=1}^{8} \frac{\partial(H_i)}{dt}. \tag{3}$$

H_i polar obstacle density of the i sector in the polar graph.

The performance evaluation is based on continuous comparison of the user tracking to the reference signals, as calculated by the obstacle avoidance system, and is given by

$$P = K_1|D_a - D_r| + K_2|S_a - S_r|. \tag{4}$$

D_a, S_a actual user travel direction and speed;
D_r, S_r recommended travel direction and speed as calculated by the OAS;
K_1, K_2 performance coefficients. These coefficients balance the "contribution" of the lateral speed offset ($|S_a - S_r|$)

and the angular offset ($|D_a - D_r|$). The values of these coefficients are determined based on several tests in which various travel patterns in different types of environments were measured. Based on these measurements the coefficients were set to $K_1 = 1.0$/deg and $K_2 = 0.5$ s/m.

The optimization procedure is performed as follows.

1) Computer simulates the expected human reaction to the transferred information (based on current models).
2) If the expected human reaction is acceptable in terms of operational requirements, the information is transmitted to the person for action. However, if the predicted reaction indicates that the person cannot achieve the desired performance (travel along the required path and avoid obstacles), the information format is modified and the process is repeated.
3) Actual human performance is recorded and evaluated.
4) Computer compares the expected performance [Step 1)] to the real performance [Step 3)] and adjusts the human model according to the differences between them. For example, if the real reaction is slower than the predicted performance, the delay time [D in (2)] is increased and the sensitivity K is reduced proportionally. If the reaction time is similar but the accuracy is different, only the sensitivity is adjusted.
5) The procedure is repeated with the adjusted model.

The prediction of human performance provides two important features.

• Computer predicts the performance and, if necessary, adjusts the information before it is relayed to the person.
• Comparing the predicted and actual performance provides a large amount of data for adjusting the human model. The computer predicts not only the final human performance, but also the transient response. Comparing the predicted and actual transient response allows the computer to adjust specific parameters in the human model (i.e., sensitivity, reaction times, etc.) rather than changing the whole model as homogeneous unit. Fig. 3 illustrates this optimization algorithm.

III. IMPLEMENTATION OF AUDITORY IMAGE SIGNALS

The *image* mode provides the user with a panoramic auditory image of the surroundings. The principle is similar to the operation of a radar system (used in air traffic control, submarines, etc.). An imaginary beam travels from the user's right ear to the left ear through the sectors covered by the *Navbelt*'s sonars (a span of $120°$ and a 5-m radius). A binaural feedback system invokes the impression of a virtual sound source moving with the beam from the right to the left ear in what we call a *sweep*. This is done in several discrete steps, corresponding to the discrete virtual direction steps. At each step, the amplitude of the signal is set proportionally to the distance to the object in that virtual direction. If no obstacles are detected by the beam, the virtual sound source is of a low amplitude and barely
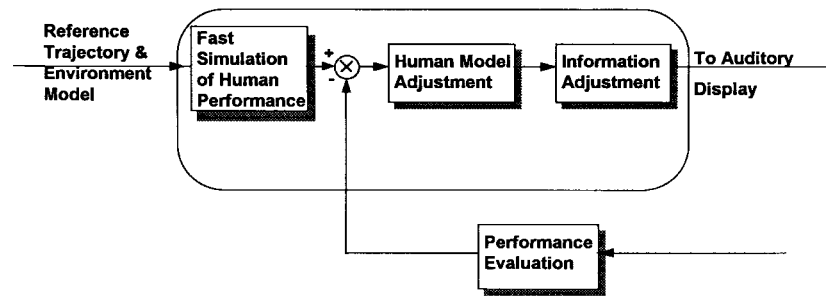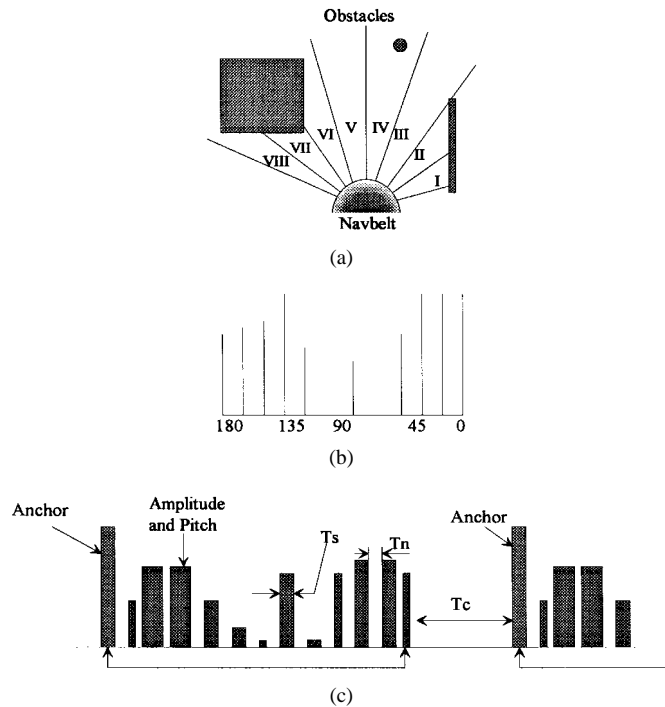
Fig. 3. Information optimization.

Fig. 4. *Image* mode: (a) obstacles are detected by the ultrasonic sensors, (b) projected onto the polar graph, and (c) an acoustic sweep is generated.

audible. If, on the other hand, obstacles are present, the amplitude of the virtual sound source is louder.

Fig. 4 demonstrates the principle of the *image* mode. Obstacles are detected by the ultrasonic sensors [Fig. 4(a)] and projected onto the polar graph [Fig. 4(b)]. Based on the polar graph, the binaural feedback system generates the *sweep*, which comprises of 12 steps [Fig. 4(c)]. Each step "covers" a sector of $15°$, so that the whole *sweep* covers a panorama of $180°$. Each of the eight sectors in the center of the panorama (covering the sectors between 30 and $150°$) is directly proportional to the corresponding sensor. The remaining four sectors (two at each side) represent sectors that are not covered by the sonars. The value of these sectors is extrapolated based on the averaged values of adjoining sectors. For example, if the third and fourth sector (representing the first and second sonar) contain an object, the first and second sectors are automatically assigned the averaged value.

Each signal is modulated by an amplitude A (indicating the distance to the obstacle in that direction), the duration T_s, for which the square wave signal is audible, and the pitch f of the square wave. The *spacing time* T_n is the length of the interval between consecutive signals during a *sweep*. After each *sweep* there is a pause of duration T_c, to allow the user to comprehend the conveyed image.

Many meaningful combinations of these parameters are possible. For example, because of the *short-term memory* capability of the human ear, a *sweep* may be as short as 0.5 s. Given enough cognition time T_c, the user will comprehend the image. Alternatively, the *sweep* time may be as long as 1 s, combined with a very short cognition time. Notice that each *sweep* starts with an anchor signal. This signal has a unique pitch, which provides the user with a convenient marker of the start of a *sweep*.

One of the important features of the *image* mode is the acoustic directional intensity (ADI), which is directly derived from the polar obstacle density histogram. The virtual direction of the ADI provides information about the source of the auditory signal in space, indicating the location of an object. The intensity of the signals is proportional to the size of the object and its distance from the person, derived from the polar obstacle density histogram. Since each sector in the histogram (H_i) reliably presents the object's density in a particular direction, the ADI does not require additional computation.

The directional intensity is a combination of the signal duration T_s, the amplitude A, and the pitch. Experiments with human auditory perception show [1] that the perceived intensity increases with the signal's amplitude, pitch, and duration. Adjusting the ADI according to the location of obstacles in the surroundings attracts the user's attention to the most relevant sections in the environment, while suppressing irrelevant data.

The information adjustment is based on updating the sweep intensity according to the human and environment models. For example, if the human reaction is unsatisfactory, the sweep transmission rate and the ADI are increased. Similarly, the transmission rate and intensity are reduced when the expected performance (calculated from the user and environment models) shows a safe and reliable travel.

IV. IMPLEMENTATION OF AUDITORY GUIDANCE SIGNALS

Implementing the *guidance* mode in the *Navbelt* is simpler than the *image* mode since the amount of transferred information is far smaller. In the *guidance* mode the computer provides the user only with the recommended travel speed and direction, based on the obstacle avoidance algorithm. The computation of the recommended travel speed and direction is similar to the computation of these parameters for a mobile robot traveling in a cluttered environment, as determined by the VFH [5]. The VFH method calculates the travel direction from the polar histogram map by searching for sections with small obstacle density. In practice, the VFH determines a threshold level, and all sections with lower obstacle density than that level become candidate sections. Next, the VFH searches for the candidate section that coincides with the direction of the target. If no candidate section coincides with the target direction, the VFH searches for the candidate section that is the closest (in terms of angular position) to the target direction. The travel speed is determined by the VFH according to the proximity of the robot (or human in the *Navbelt*) to the nearest object. The speed is determined inversely proportional
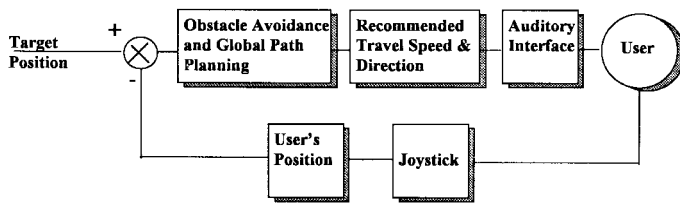
Fig. 5.   Schematic description of the simulator.

Fig. 6.   Typical transient response in tracking by auditory localization.

to the minimal distance, with a maximum speed of 1.2 m/s, attained when the distance between the traveler and the closest object is larger than 3 m.

The recommended travel speed and direction are relayed to the user by a single stereophonic signal. The virtual direction of the signal is the direction the obstacle avoidance system has selected for travel. The pitch and amplitude are proportional to the recommended travel speed. Higher pitch and amplitude attract more human attention [1], thereby motivating the traveler to reduce the walking speed and concentrate on the stereophonic signal. A special low-pitch signal (250 Hz) is transmitted when the direction of motion coincides (within $\pm 5°$) with the required direction. This special tone is a simple feedback signal for the user, indicating that the travel direction is correct. Furthermore, low-pitch tones occlude external sound from the environment less than medium- and high-pitch tones [1]. The higher pitch tone is transmitted only when the traveler needs to change the travel direction, and as soon as that direction coincides with the recommended direction, the low-pitch returns.

Another important parameter involved in the guidance mode is the rate at which signals are transmitted. Although a low transmission rate causes less occlusion of external sounds, it may also be too slow to alert the traveler to hazards. The adaptive information transfer system adjusts the transmission rate according to changes in the process and the user's requirements, similar to the way the information flow is adjusted in the *image* mode. When the user is traveling in an unfamiliar environment cluttered with a large number of obstacles, the transmission rate increases and may reach up to ten signals per second. On the other hand, when traveling in an environment with few or no obstacles, the transmission rate is reduced to one signal every 3 s.

V. EXPERIMENTS WITH THE *Navbelt* SIMULATOR

To evaluate the *Navbelt* concept under different conditions, a simulator was developed. The simulator is based on the same hardware as the *Navbelt* and the same acoustic signals that guide the user with the real *Navbelt*. The user's response to these signals is relayed to the computer by a joystick. Several maps are stored in the computer's memory, representing different types of environments with different levels of travel complexity. Some of the maps were constructed from real sonar data gathered with a mobile robot during travel. Other maps were generated by the computer. In the experiments with the simulator, subjects "traveled" through the different maps while listening to the sounds generated by the computer. A schematic description of the simulator is shown in Fig. 5.

During the development stages, the simulator was used to investigate the effect of different auditory signals on human performance. However, the simulator can also be used as an efficient tool for training new users. The simulator can provide practice runs through different types of environments with absolutely no risk to the user. User performance can be recorded and help in the analysis of an individual's progress and the effectiveness of certain training procedures.
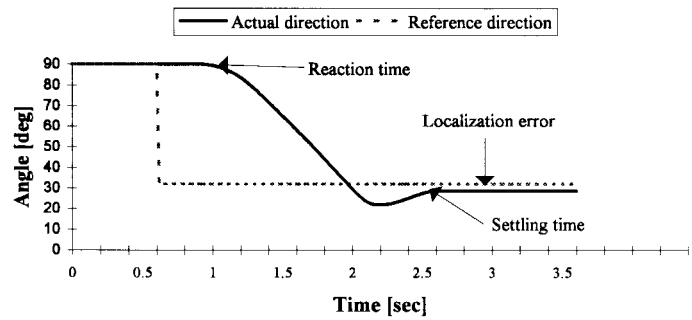
A. Experiment #1) Transient Response in Auditory Localization

In this experiment, the transient response of humans in tracking by auditory localization was investigated to verify the human model (2) for aural compensatory tracking and adjust information flow according to operational requirements and the expected human reaction. Subjects listened to stereophonic signals through headphones. The stereophonic signals were randomly generated by the computer, varying in their virtual direction, pitch, amplitude, length, and the rate at which they were transmitted. The subject's goal was to position the joystick at the direction of the virtual sound source. The joystick was modeled as a first-order system with a time constant of $\tau = 0.667$ s and a unit gain. Eight subjects were included in this experiment, all sighted with good hearing capabilities. The subjects' ages ranged from 18 to 35. Each session included 5 min of practice, followed by 15 min of experiments and 10 min of rest. Each subject was tested in 400 runs. The parameters involved in transferring the stereophonic signals were selected randomly by the computer to reduce the effect of learning or to get used to a particular format of information. However, only two parameters were changed in each test. One parameter was the virtual direction, and the other was selected randomly by the computer (pitch, amplitude, length, or transmission rate). Fig. 6 describes a typical transient response for tracking by auditory localization. As shown, the response includes a reaction time—the time required to perceive and analyze the incoming signals, a settling time—the time it takes to reach the desired position, and an offset that indicates the accuracy of the test.

The results from all subjects were combined and then classified according to the different variables. Results were also filtered by a low-pass filter to reduce the effect of noise. Fig. 7 describes some of the results from these tests.

Discussion: According to the results, two parameters have a major effect on the localization error: the signal's frequency and the signal's amplitude. The localization error is smaller for frequencies between 400 and 1000 Hz, with the minimal error around 800 Hz. This result is consistent with similar experiments [7] investigating the performance of pilots in localization of auditory signals in the cockpit. Our results are also consistent with theoretical research [1], [14], which concluded that low frequencies (below 2 kHz) contribute mainly to a sense of localization, while high frequencies contribute more to the broadening of the auditory event. The lower error for lower amplitudes is also consistent with experiments performed by Benson [1], which showed that the stereophonic localization is better perceived for lower amplitudes (less than 20 dB).

The reaction time (RT) is affected, according to our results, by the transmission rate only. The RT is kept constant around 700 ms for all signals' amplitudes and frequencies, increased slightly for transmission rate between 2 and 5 Hz (to 800 ms), and from there on increased significantly with lower transmission rates. This
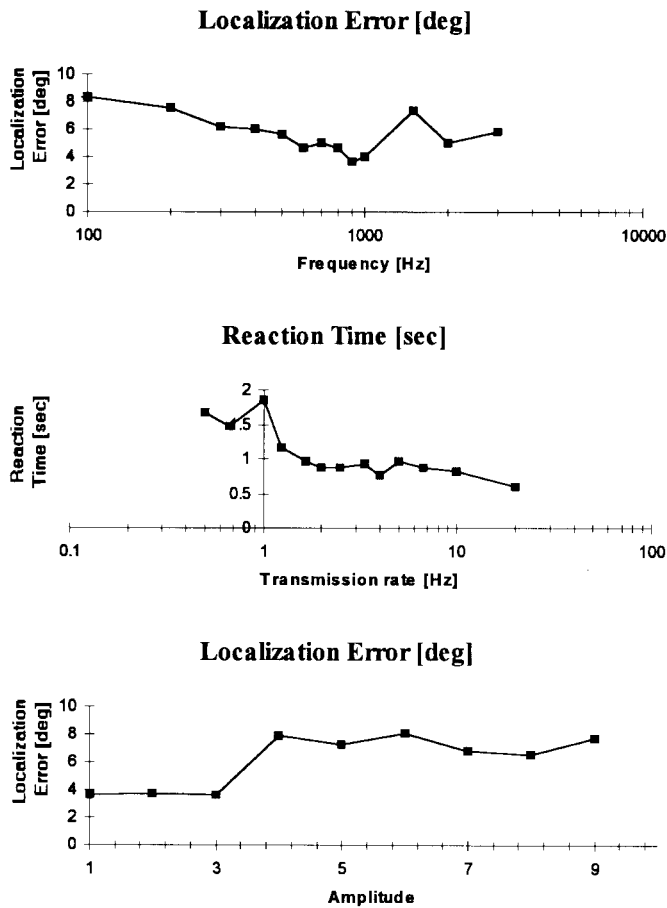
Fig. 8. Schematic description of Experiment #2.

Fig. 7. Effect of changes in pitch on transient response.

Fig. 9. Effect of changes in workload on transient response.

result is expected since with low transmission rates; there are long delays between each transmission. Like the reaction time, the settling time (ST) is not affected by changes in frequency or amplitude, but it increases significantly with transmission rates lower than 1.25 Hz. The reason is similar to the increased reaction time in low transmission rates.

B. Experiment #2) Investigation of Workload in Auditory Localization

In the second experiment, the workload involved in auditory localization was investigated. Fig. 8 is a schematic illustration of this experiment. Subjects were performing the localization task, as in Experiment #1. However, an additional task was introduced. The computer generated high- and low-pitch tones (458 and 225 Hz) and subjects were asked to press a key according to the transmitted tone. The motivation behind this experiment was to introduce a secondary task that involved perception of the same modality as the main task (auditory) and required some cognition (indicating the type of tone). The effects of adding a secondary task to the localization process is important because blind travelers are expected to interact with the surroundings while walking (i.e., talk to other people, listen to external acoustic signals, etc.), which is the equivalent of the secondary task.

The frequency at which the tones were introduced to the subjects varied randomly, again reducing the effect of learning or adjusting to a particular pattern. The tones were displayed until the subject pressed the right key. Before starting the experiment, a benchmark test was conducted to evaluate the performance of each subject on the second task only. When performing the two tasks simultaneously,
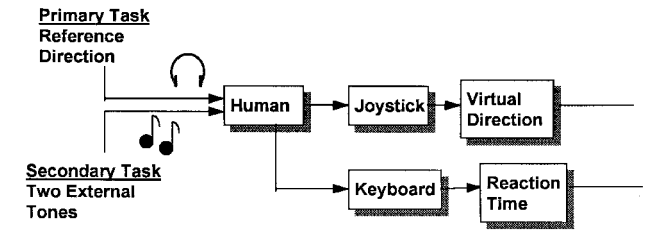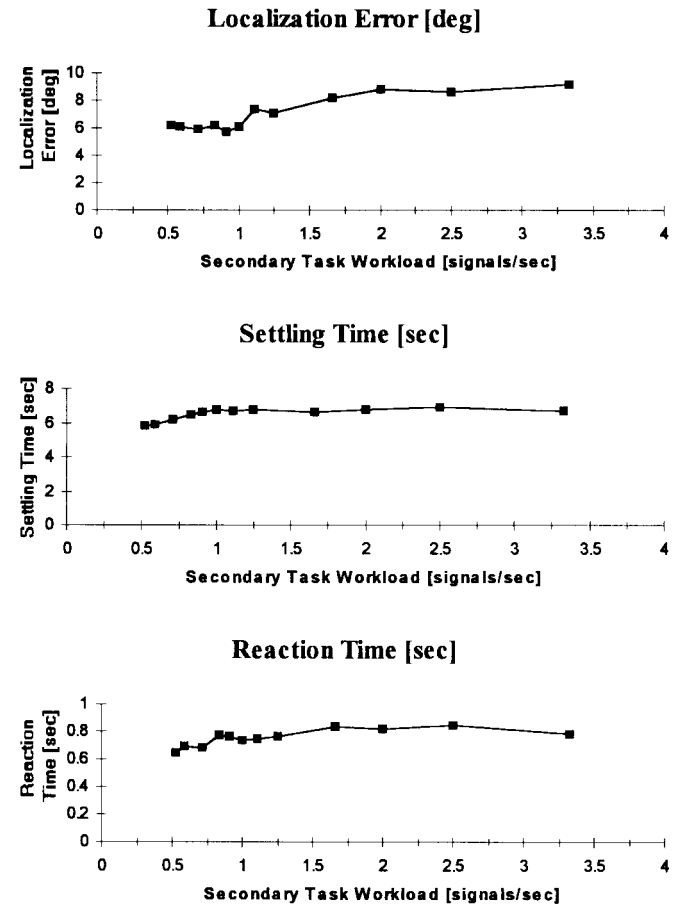
subjects were asked to perform their best on the secondary task, so that reduction in performance due to the additional workload would affect the primary task only. The results of this experiment are described in Fig. 9.

Discussion: The localization error was significantly reduced due to changes in the workload. When the tones of the secondary task were introduced at a rate of 3.33 Hz (a new tone every 330 ms), the localization error was around 10°. However, as the workload was gradually reduced to 1 Hz (one tone/s), the localization error was reduced by 40% (to about 6°). RT and ST were also affected, but the changes were more moderate. RT was reduced from 850 ms, with 3.33 Hz of the secondary task, to around 700 ms, with 1 Hz of the secondary task (18%), and ST was reduced from 6.9 to 6.1 s (12%).

C. Experiment #3) Investigation of Reaction to a Single Obstacle

The motivation behind this experiment was to investigate the human performance for basic obstacle configuration. The experiment was conducted with the *Navbelt* simulator using a simple single

TABLE I
RESULTS SUMMARY—TRAVEL SPEED [cm/s]. *EXPERIENCE—SUBJECT WITH 40-h
EXPERIENCE; NO EXPERIENCE—SUBJECT WITH LESS THAN 20-h EXPERIENCE

	Single object	Different maps	*Navbelt prototype	
			Experience	No Experience
Adaptive Guidance	99	77	80	65
Regular Guidance	99	64	65	45
Adaptive Image	89	52	50	30
Regular Image	82	40	45	30
Visual	105	—	—	—
Visual Image	92	—	—	—

object. The subject's position and orientation was shown on the computer monitor, along with the target position. For each run, the computer generated an individual simulated obstacle at a random location and at a random time. However, the obstacle was wide enough to block the path between the subject and the target, therefore, requiring a change in the travel direction. The experiment included six different formats of object presentation, as follows.

1) Adaptive *Guidance* Modes—the recommended auditory travel direction is presented, with adaptation of the rate amplitude and frequency according to the human model.
2) Regular *Guidance* Mode—the recommended auditory travel direction is presented at a rate of 1 Hz, with a fixed amplitude and frequency (800 Hz).
3) Adaptive *Image* Mode—adjusted according the human model.
4) Regular *Image* Mode—presented at a fixed rate (1 Hz).
5) Visual mode in which the actual obstacle was displayed on the screen.
6) Visual *image* mode, in which the polar histogram map was presented.

Several parameters were measured in this experiment, as follows.

- **Reaction Time**—the time from displaying the obstacle until the subject starts changing the travel path to avoid it.
- **Speed**—average travel speed.
- **Accuracy**—deviation from the recommended direction.
- **Unsuccessful Trials**—the percentage of collisions with objects.

Some of the results (travel speed) are summarized in Table I.

Discussion: The most obvious conclusion from this experiment is that none of the auditory displays is as good as visual display for obstacle avoidance. Examining the most important parameter, the percentage of unsuccessful trials, shows that the best auditory display—the adaptive guidance mode—had three times more collisions than the visual display (18 versus 6%) and 40% more collisions than the *visual image* display. However, another important conclusion is that the adaptation of information transfer by the system for all auditory displays improves human performance. These adaptations improved user reaction time in the *guidance* mode by 45% and reduced unsuccessful trials by 25%. In the *image* mode, the adaptation improved reaction time by 8%, speed by 6%, and reduced unsuccessful trials by 21%.

D. Experiment #4) Simulations in Different Types of Environments

To investigate the performance of the *Navbelt* simulator in different environments, virtual maps were constructed by the computer. Some maps were based on real data collected by a mobile robot, while others were generated by the computer. Ten maps, stored in the

computer, were selected randomly to reduce the effect of learning the maps.

In the experiments with the *image* mode, the position of the subject and the location of the target were shown on the computer screen. When subjects "collided" with an obstacle, a verbal message informed the subject about the collision, and no forward travel was permitted. The subject then "turned" or "backed up" to continue traveling toward the target. After reaching the target, the full map was superimposed on the traveling path so that the subject's performance during the run could be evaluated.

In the experiment with the *guidance* mode, only the traveler's simulated position was shown on the screen, while the target position was unknown to the subject. This is the equivalent of traveling in an unfamiliar environment, where the traveler depends entirely on the guiding signals from the *Navbelt*. As with the *image* mode, when subjects "collided" with an obstacle, a verbal message informed the subject about the collision and no forward travel was permitted. The target position was selected randomly by the computer to simulate travel in unfamiliar environments toward unknown targets. The subject's goal was to "travel" from the initial position to the target. Subject performance was continuously monitored and recorded according to the mobility assessment described previously (4).

The experiment included 1200 tests, in which each one of the operation modes was tested 600 times, divided equally between all subjects. Since the maps were different in their level of complexity (in terms of obstacle avoidance), each map was tested 30 times in each display mode. Table I summarizes the average travel speeds in this experiment.

Discussion: The results of this experiment show the improvement in mobility performance achieved by the adaptive information transfer architecture. The travel speed with adaptation was increased by 29% in the *guidance* mode and 18% in the *image* mode compared with nonadaptive displays. The improvement in the directional error was 5.1% in the *guidance* mode and 0.9% in the *image* mode. The fastest average traveling speed was achieved using the *guidance* mode in map 2 (0.95 m/s), while the slowest speed was in *image* mode traveling through map 10 (0.31 m/s). Map 2 simulates an open space with no obstacles at all, while map 10 simulates a crowded street with many obstacles positioned in random order.

Analysis of the results of the fastest and slowest maps, as well as of the travel speeds achieved in all other maps, indicates that the *Navbelt* is particularly effective in environments with low obstacle density. This can be explained as follows. When traveling in complex environments with many obstacles, the amount of information required for safe travel is large, especially with the *image* mode. Even with adaptive information transfer, the richness of the information exceeds the bandwidth of the system, which is limited by the human's slow rate of comprehension. However, when traveling in an easy environment with only a few obstacles, the *Navbelt* is advantageous, as its sensors provide a wide coverage of the surroundings and the information relayed to the traveler requires little conscious effort. The extended coverage of the *Navbelt*, mainly its "preview" distance, increases the traveler's confidence, which results in a higher travel speed. Research on the effect of nonvisual preview upon the walking speed of visually impaired people [6] showed that a preview of 3.5 m using a Sonic Pathsounder [8] increased walking speed by 18% compared to travel speed with the long cane. The *Navbelt* provides not only a long but also a wide preview, thus providing the traveler with extra time to take the necessary actions to avoid obstacles.

VI. EXPERIMENTS WITH THE *Navbelt* PROTOTYPE

The major problem in conducting experiments with the *Navbelt* prototype is the lack of a reliable position feedback system. Reliable
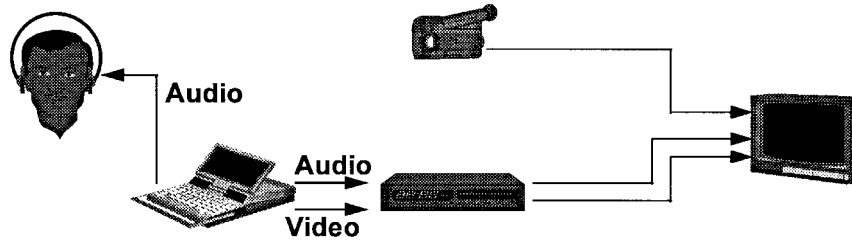
Fig. 10. Feedback system for laboratory experiments.

position feedback systems are usually complex, expensive, and confined to a specific location. To reduce the complexity of the position feedback system in the *Navbelt* prototype while maintaining reliable data, an audio-visual system, described in Fig. 10, was developed. In this system, the subject's motion is recorded by a video camera. In addition, the computer data are directly recorded by a VCR. The stereophonic signals transmitted to the user are also recorded by the VCR. The image from the video camera is then superimposed with the computer image from the VCR, resulting in a display that includes the environment, human motion, computer data, and the acoustic signals relayed to the user.

In the initial experiments with the *Navbelt* prototype, subjects were traveling in the controlled environment of the laboratory through various obstacle courses, using the different modes of operation. In the first experiment, vertical poles with different diameters were positioned along the travel path. It was found that the *Navbelt* could detect poles as thin as 10 mm in diameter. However, detection was reliable only if the objects were stationary and the subject was traveling slowly and smoothly. When either the thin poles were moved at a speed of 0.5 m/s, or when the subject walked faster than 0.5 m/s, the obstacle avoidance system could not detect the poles. Also, sudden changes in the travel direction caused the system to miss some of the thin poles. However, the *Navbelt* reliably detected objects with a diameter of 10 cm or bigger, regardless of the travel speed.

The next experiment was aimed at evaluating the *Navbelt*'s reliability in terms of walking patterns. It was found that uneven walking patterns cause the sonars to swing along the vertical plane, which reduces the *Navbelt*'s performance. In addition, it was found that the relative angle between the sonars and the vertical orientation of the *Navbelt* (the angle of the sonars with the horizon) had a significant effect on object detection. For example, if the *Navbelt* is tilted by 5° from the horizon, the sonar reading can be off by more than 9%. Swinging the arms during a normal walking pattern did not interfere with the sonar performance, as no sonars are directed to the sides. Using the White Cane (the most common device used by blind travelers) can cause interference to the sonar performance, mainly when it is used to detect objects above the ground level (higher than 0.5 m). However, since the cane is used mainly to detect objects at ground level, while the *Navbelt* is designed to detect objects above ground level, this interference is not critical to the general performance.

Based on the results of this experiment, the first prototype was modified to have a more rigid structure. The modified prototype is designed to be tightly fastened to the user's waist to minimize oscillations, even with an uneven walking pattern. The rigid structure guarantees that the sonar maintain accurate readings, even in case of a collision.

Once subjects were confident with the *Navbelt* prototype, supervised experiments in "real-world" environments were conducted. Subjects traveled outside buildings, detecting and avoiding common objects, such as trees, parked cars, walls, bicycles, and other pedestrians. Other tests were conducted inside office buildings, where subjects traveled along corridors, located doors and curves, and detected

and avoided furniture. One of the major concerns of users was the limitation of the prototype in detecting overhanging objects, steps, road curbs, etc. However, future improvements include adding more sonars pointing up and down to detect these type of objects.

Although no special experiments were conducted to investigate the effect of stress and fatigue, all subjects stated that the *image* mode is far more demanding than the *guidance* mode in terms of perceptual and cognitive load, therefore, they prefer to use the *image* mode only for short periods of time. However, blind people stated that they prefer the *image* mode unless traveling in a known environment. Blind travelers prefer to stay "in the loop" as much as possible. The *image* mode provides information about the location of objects, and the global path planning and obstacle avoidance tasks are performed by the user.

The experiments with the *Navbelt* prototype showed the importance of training. Subjects with more experience traveled faster and generally felt more comfortable with the *Navbelt*. After 20 h of practice with the *Navbelt* simulator and 40 h of practice with the prototype, the average travel speed was 0.8 m/s in the *guidance* mode and 0.5 m/s in the image mode. Subjects with less experience (10 h with the simulator and 10 h with the prototype) traveled at an average speed of 0.6 m/s in the *guidance* mode and 0.3 m/s in the *image* mode. Table I provides details about the travel speeds in these experiments.

VII. CONCLUSIONS

Techniques used in mobile robot obstacle avoidance systems have been transferred successfully to a navigation aid for the blind. Instead of transmitting electronic signals to the robot motion controllers, the obstacle avoidance system relays information to the user by transmitting stereophonic signals. These signals provide spatial information about the location of objects in the environment, or guidance information for the recommended travel direction and speed.

This method is implemented in a new travel aid for the blind, the *Navbelt*. Blindfolded subjects traveling with the *Navbelt* prototype through cluttered environments could walk as fast as 0.8 m/s using the *guidance* mode.

One of the important observations in the experiment with the *Navbelt* simulator and prototype was that extended practice had a substantial effect on performance. Although this aspect was not formally investigated in this paper, it was clear that subjects with extensive practice performed better than subjects with little practice.

REFERENCES

[1] B. Benson, *Audio Engineering Handbook.* New York: McGraw-Hill, 1986.
[2] B. Blasch, R. G. Long, and N. Griffin-Shirley, "National evaluation of electronic travel aids for the blind and visually impaired individuals: Implications and design," in *Proc. RESNA 12th Annu. Conf.,* New Orleans, LA, June 1989, pp. 133–134.
[3] J. Borenstein, "The *Navbelt*—A computerized multi-sensor travel aid for active guidance of the blind," in *Proc. CSUN's 5th Annu. Conf. Technol. Persons Disabilities,* Los Angeles, CA, Mar. 21–24, 1990, pp. 107–116.

[4] J. Borenstein and Y. Koren, "Noise rejection for ultrasonic sensors in mobile robot applications," in *Proc. IEEE Conf. Robot. Automat.,* Nice, France, May 1992, pp. 1727–1732.

[5] ——, "The vector field histogram—Fast obstacle avoidance for mobile robots," *IEEE J. Robot. Automat.,* vol. 7, pp. 278–288, June 1991.

[6] D. Clark-Carter, A. D. Heyes, and C. I. Howarth, "The efficiency and walking speed of visually impaired people," *Ergonomics,* vol. 29, no. 12, pp. 1575–1581, 1986.

[7] A. Ericson and R. L. Mckinley, "Auditory localization cue synthesis and human performance," in *IEEE Proc. Nat. Aerosp. Electron. Conf.,* NASEA9, 1989, vol. 2, pp. 718–725.

[8] L. Kay, "A sonar aid to enhance spatial perception of the blind: Engineering design and evaluation," *Radio Electron. Eng.,* vol. 44, no. 11, pp. 605–627, 1974.

[9] D. T. McRuer, D. Graham, E. S. Krendel, and W. Reisener, "Human pilot dynamics in compensatory systems," AFFDL-TR-65-15, 1965.

[10] A. Shoval, J. Borenstein, and Y. Koren, "The *Navbelt*—A computerized travel aid for the blind," in *Proc. RESNA Conf.,* Las Vegas, NV, June 13–18, 1993, pp. 240–242.

[11] S. Shoval, "Integration of intelligent agents in an adaptive aiding system for the blind," Ph.D. dissertation, Dept. Mech. Eng. Appl. Mech., Univ. Michigan, Ann Arbor, 1994.

[12] S. Tachi, R. W. Mann, and D. Rowel, "Quantitative comparison of alternative sensory displays for mobility aids for the blind," *IEEE Trans. Biomed. Eng.,* vol. BME-30, pp. 571–577, Sept. 1983.

[13] E. W. Vinje and E. T. Pitkin, "Human operator dynamics for aural compensatory tracking," in *Proc. 7th Annu. Conf. Manual Contr.,* Los Angeles, CA, 1971.

[14] Y. Yost and C. S. Watson, *Auditory Processing of Complex Sounds.* Hillsdale NJ: Lawrence Erlbaum, 1989.

A Nonrecursive Newton–Euler Formulation for the Parallel Computation of Manipulator Inverse Dynamics

Jing Jun Zhang, You Fang Lu, and Bin Wang

Abstract—This paper focuses on the inverse dynamics formulation of manipulators that is suitable for parallel computation, and a corresponding nonrecursive Newton–Euler formulation is presented. In order to illustrate its potential parallelism, a simple parallel scheduling scheme is proposed, and the parallel computational efficiency for the inverse dynamics of the basic three links of a PUMA 560 robot is analyzed. Compared with other algorithms, the theoretical computation cost of this parallel algorithm, in which factors such as communications overhead are ignored, is smaller.

Index Terms—Inverse dynamics, manipulators, parallel algorithm.

I. INTRODUCTION

The so-called manipulator inverse dynamics problem is to calculate the joints forces or torques to achieve a given motion trajectory. In control applications, the computation of inverse dynamics is

usually incorporated as an element of the feedback or feedforward path to convert the positions, velocities, and accelerations, computed according to some desired trajectory, into the joint generalized forces that will achieve those accelerations. In trajectory planning, inverse dynamics can be used to ensure that a proposed trajectory can be executed without exceeding the actuators' limits. The computation of inverse dynamics is also used as a building block for constructing forward dynamics algorithms, which are useful in performing dynamic simulations of robot manipulator [1].

For achieving the convergence of the control algorithm and real-time control, the computation of inverse dynamics must be performed online and repeated very frequently, preferably at a sampling rate of no less than 60 Hz, since the resonant frequency of most of the mechanical manipulators are around 10 Hz [2]. Furthermore, from the servo-control point-of-view, a more realistic criterion is the 300-Hz sampling rate for controlling the PUMA robot [3]. Therefore, the fast computation scheme for manipulator inverse dynamics is desirable.

A number of serial inverse dynamics formulations have been developed over the last few years, among which the recursive Lagrangian formulation [4] and the recursive Newton–Euler formulation [2] are the most significant algorithms. He and Goldenberg [5] presented another algorithm to further improve the efficiency of the inverse dynamics by use of the concepts "augmented body" and "barycenter." Further substantial improvement in computational efficiency, however, is unlikely to be achieved, since the existing serial algorithms possess the time lower bound of $O(n)$. Nevertheless, some improvement could be achieved by parallel computations [6].

There are two approaches for mapping a problem onto parallel architectures. In the first approach, a target architecture is initially considered. An algorithm is then developed to exploit its parallelism, and the computational model is supported by the architecture. The drawback of this approach is that the architecture features and the topological variation will limit the algorithm's performance. Another approach, which is also a standard approach in the parallel computation of manipulator dynamics, is to develop an algorithm to efficiently exploit parallelism in the problem. An algorithmically specialized parallel architecture is then designed to support the algorithm [7]. In general, a parallel algorithm includes a computational formulation and parallel scheduling scheme based on the formulation.

Luh and Lin [8] presented a variable branch-and-bound search to find an optimal subtask-ordered schedule for each of the processors. It is assumed that one processor is assigned to each manipulator link and that the data can be transferred between the adjacent processor only. Lathrop [9] proposed two parallel algorithms using special-purpose processors. The first is a linear parallel algorithm that is related to the Luh and Lin method [8]. The second is a logarithmic parallel algorithm based on the partial sum technique. Kasahara and Narita [10] introduced a parallel processing scheme using two scheduling algorithms: depth first/implicit heuristic search and critical path/most immediate successors first. It is assumed that data can be transferred among all processors. Lee and Chang [6] proposed a parallel algorithm based on the recursive doubling technique with a modified inverse perfect shuffle interconnection scheme between a set of processors. Vukobratovic *et al.* [11] developed a parallel algorithm using a modified branch-and-bound method combined with the largest processing time first algorithm. Chen *et al.* [12] presented two algorithms, the A^* and the dynamic highest level first/most immediate successors first. Lee and Chen [13] developed two efficient mapping algorithms for scheduling the execution of the